

國立交通大學

電信工程學系

碩士論文

應用於無線干擾環境下結合時空編碼
技術及展頻系統之研究

Combined Space-Time Coding with
Frequency-Hopping Spread Spectrum for
Wireless Jamming Channels

研究生：陳宗保

指導教授：王忠炫 博士

中華民國九十六年九月

應用於無線干擾環境下結合時空編碼
技術及展頻系統之研究

**Combined Space-Time Coding with
Frequency-Hopping Spread Spectrum for
Wireless Jamming Channels**

研究生：陳宗保

Student: Chung-Pao Chen

指導教授：王忠炫

Advisor: Chung-Hsuan Wang

國立交通大學

電信工程學系碩士班



A Thesis

Submitted to Department of Communication Engineering
College of Electrical and Computer Engineering
National Chiao Tung University
in Partial Fulfillment of the Requirements
for the Degree of
Master of Science
in
Communication Engineering

September, 2007

Hsinchu, Taiwan, Republic of China

中華民國九十六年九月

應用於無線干擾環境下結合時空編碼 技術及展頻系統之研究

學生：陳宗保

指導教授：王忠炫

國立交通大學電信工程學系碩士班

摘要

在無線傳輸的環境中，傳輸的信號常遭受到惡意的干擾源及通道衰減效應，導致接收訊號產生嚴重的失真。跳頻展頻系統是一般最常用來抑制干擾效應的技術，而具有分集增益及編碼增益的時空編碼技術可有效的降低通道衰減效應。因此，在本篇論文裡吾人便結合了兩者之優點，提出了時空編碼結合跳頻展頻技術以提升傳輸系統在無線干擾環境中之整體效能。

為了能夠專注於分析時空碼的解碼設計，吾人考慮了三種較簡單的跳頻方式。第一種定義為所有傳送天線的信號都跳至相同的頻帶上，稱此為最差跳頻。第二種情形為所有傳送信號皆設計為避免互相發生碰撞，稱此為最佳跳頻。而最後一種所提出的跳頻方式，便是任何傳輸信號皆隨機的跳至任一頻帶上，稱此為均勻跳頻。其中最差及最佳跳頻方式分別代表為此系統效能分析的上界與下界。而在跳頻頻帶數夠大及傳送天線個數少的情況下，均勻跳頻方式可使系統效能近似於使用最佳跳頻方式。針對上述跳頻方式，吾人推導出在路徑增益已知或未知情況下此系統的最大可能性解碼。然而，由於最大可能性解碼相當的複雜，在實際應用中較不易實現，因此，吾人提出了一些次佳解碼方式來降低解碼複雜度，並模擬其在多重傳送及接收天線架構下之效能。此外，吾人亦針對此系統提出了在無線干擾環境下好的時空碼準則。最後經由模擬結果驗證出，在相同的訊雜比及頻寬效益的考量之下，此系統比傳統單進單出編碼效能來的更佳。

Combined Space-Time Coding with Frequency-Hopping Spread Spectrum for Wireless Jamming Channels

Student: Chung-Pao Chen

Advisor: Chung-Hsuan Wang

Department of Communication Engineering

National Chiao Tung University

Abstract

In wireless jamming environments, the transmitted signals usually suffer from hostile jammers and undesired channel impairments, e.g., multipath fading. Conventionally, frequency-hopping spread spectrum (FHSS) systems are most effective anti-jamming techniques, and space-time coding (STC), which introduces temporal and spatial correlation into the transmitted signals to achieve transmitter diversity without sacrificing the bandwidth, has been shown to provide excellent performance against multipath fading. Therefore, in this thesis, we combine STC with the FHSS to construct a powerful high-rate transmission scheme for wireless jamming channels.

Three cases of FH are considered here to simplify the design of STC. One is the worst-case frequency hopping which hops the symbols from all transmitter antennas into the same frequency band, another is the perfect frequency hopping which avoids any possible collision of the transmitted symbols, and the other is the uniform frequency hopping which hops the transmitted symbol randomly over the total frequency hopping bands. The actual performance of the combined STC/FHSS system with arbitrary hopping patterns can then be upper and lower bounded by the evaluated performance of the worst case and perfect case, respectively. Moreover, the performance of the uniform case can approach the perfect case as the number of frequency bands is very large and few antennas are used for transmission. The maximum likelihood decoding of space-time codes is derived with respect to different reception conditions. Several suboptimal schemes are proposed for complexity reduction.

We also present the design criteria for constructing good space-time codes with respect to the wireless jamming channels. Verified by the simulation results, the proposed system can provide better performance than the conventional schemes in terms of both bandwidth efficiency and signal-to-noise ratio.



誌謝

時光匆匆而過，回首兩年的研究生活，真是讓我人生成長了不少，首先要感謝指導老師王忠炫老師，兩年來不斷的在研究上給予細心的指導與教誨，使我在學識上及做事的態度上成長不少、受益匪淺，感謝您！除此之外，亦要感謝實驗室的夥伴們：大師兄，謝謝你總是在我研究遇到瓶頸時，總是很熱心的協助我，給予幫助。賴桑、慶和和老宋，從你們身上我學到很多看待事物不一樣的觀點。同屆的仁哥和小民，感謝你們啦！因為有你們的陪伴，彼此支持鼓勵，兩年來受你們照顧很多。學弟小白、阿尼、老菜、和一哥，總是在我最需要的時候給予歡笑和關懷，一同聊天打屁，真的是一群可愛的學弟喔！還有謝老師實驗室的強哥、宏益、小湯，常常一起去游泳及健身，紓解壓力，很謝謝你們的陪伴。DUCK、施施、振偉及冠亨，謝謝你們，有你們在真好！還有慈青社的夥伴，常給我精神上的支持。最後，要感謝我的家人們，總是默默的陪伴，給予鼓勵與支持。一起分享生活的評兒，兩年來互相打氣鼓勵，感謝妳。因為有你們的陪伴與支持，我的人生充滿了色彩，感謝你們！下個人生階段，我會更加努力的！



Contents

Chinese Abstract	I
English Abstract	II
Acknowledgement	IV
List of Figures	VIII
List of Tables	XII
1 Introduction	1
2 Overview of Frequency-Hopping Spread Spectrum Systems and Jamming Environments	4
2.1 FHSS Systems	4
2.2 Jamming Environments	5
2.2.1 Broadband Noise Jammers	6
2.2.2 Partial-Band Noise Jammers	7
2.2.3 Multitone Noise Jammers	9
3 Review of Space-Time Coding	14
3.1 STC System Model	14
3.2 Encoder Structure for STTC	15
3.3 Maximum Likelihood Decoding	16
3.4 Design Criteria for Constructing Good Space-Time Codes	17



4	STC Combined with FHSS in Quasi-Static Fading Channels	21
4.1	STC/FHSS System Model	22
4.2	STC Combined with Worst-Case FH	27
4.2.1	Decoding with CSI Available	27
4.2.1.1	Maximum Likelihood Decoding with JSI Available	27
4.2.1.2	Suboptimal Decoding Schemes	28
4.2.2	Decoding without CSI	29
4.2.2.1	Maximum Likelihood Decoding with JSI Available	29
4.2.2.2	Suboptimal Decoding Schemes	31
4.2.3	Design Criteria for Constructing Good Space-Time Codes	33
4.3	STC Combined with Optimum FH	35
4.3.1	Decoding with CSI Available	36
4.3.1.1	Maximum Likelihood Decoding with JSI Available	36
4.3.1.2	Suboptimal Decoding Schemes	37
4.3.2	Decoding without CSI	38
4.3.2.1	Maximum Likelihood Decoding with JSI Available	38
4.3.2.2	Suboptimal Decoding Schemes	38
4.3.3	Design Criteria for Constructing Good Space-Time Codes	41
4.4	STC Combined with Uniform FH	43
4.4.1	Decoding with CSI Available	44
4.4.1.1	Maximum Likelihood Decoding with JSI Available	44
4.4.1.2	Suboptimal Decoding Schemes	45
4.4.2	Decoding without CSI	45
4.4.2.1	Maximum Likelihood Decoding with JSI Available	45
4.4.2.2	Suboptimal Decoding Schemes	47
4.5	Simulation Results and Discussions	49
5	Conclusions	70

A Independent of the Jamming Noise in Time, Frequency, and Space Domains	72
B Derivation of the ML Decoding of STC/WFHSS Systems without CSI	75
C Derivation of the Design Criteria of STC/WFHSS Systems	82
D Derivation of the ML Decoding of STC/OFHSS Systems without CSI	88
E Derivation of the Design Criteria of STC/OFHSS Systems	90
F Derivation of the ML Decoding of STC/UFHSS Systems without CSI	95
Bibliography	99



List of Figures

2.1	FH/MFSK system model.	5
2.2	Power spectral density of broadband noise jammer.	6
2.3	Power spectral density of partial-band noise jammer.	8
2.4	Performance of FH/BFSK system in partial-band noise jamming environment for different factors ρ	9
2.5	Power spectral density of multitone noise jammer.	10
2.6	Band multitone noise jammer and independent multitone noise jammer strate- gies.	10
2.7	Performance of FH/MFSK in several different jamming environments.	13
3.1	STC system model.	14
3.2	The encoder of STTC system for two transmitter antennas	16
4.1	The proposed STC/FHSS system.	22
4.2	STC/WFHSS system model	23
4.3	STC/UFHSS system model	24
4.4	Example of the STC/UFHSS system for selected receiver signals	26
4.5	STC/OFHSS system model	26
4.6	Performance plots of STC/WFHSS with CSI available for $\rho = 0.2$ and $E_b/N_0 = 15$ dB.	52
4.7	Performance plots of STC/WFHSS with CSI available for $\rho = 0.05$ and $E_b/N_0 = 15$ dB.	52

4.8	Performance plots of STC/OFHSS with CSI available for $\rho = 0.2$ and $E_b/N_0 = 15$ dB.	53
4.9	Performance plots of STC/OFHSS with CSI available for $\rho = 0.05$ and $E_b/N_0 = 15$ dB.	53
4.10	Performance plots of STC/UFHSS with CSI available for $\rho = 0.2$ and $E_b/N_0 = 15$ dB.	54
4.11	Performance plots of STC/UFHSS with CSI available for $\rho = 0.05$ and $E_b/N_0 = 15$ dB.	54
4.12	BER v.s. ρ of the ML decoding of STC/WFHSS for $E_b/N_0 = 25$ dB with CSI available.	55
4.13	3-dimension plots of the BER v.s. ρ for the ML decoding of STC/WFHSS for $E_b/N_0 = 25$ dB with CSI available.	55
4.14	BER v.s. ρ of the ML decoding of STC/WFHSS for $E_b/N_0 = 15$ dB with CSI available.	56
4.15	3-dimension plots of the BER v.s. ρ for the ML decoding of STC/WFHSS for $E_b/N_0 = 15$ dB with CSI available.	56
4.16	BER v.s. ρ of the ML decoding of STC/OFHSS for $E_b/N_0 = 15$ dB with CSI available.	57
4.17	3-dimension plots of the BER v.s. ρ for the ML decoding of STC/OFHSS for $E_b/N_0 = 15$ dB with CSI available.	57
4.18	BER v.s. ρ of the ML decoding of STC/UFHSS for $E_b/N_0 = 15$ dB with CSI available.	58
4.19	3-dimension plots of the BER v.s. ρ for the ML decoding of STC/UFHSS for $E_b/N_0 = 15$ dB with CSI available.	58
4.20	BER v.s. ρ of the ML decoding of STC/WFHSS for $E_b/N_J = 10$ dB with CSI available.	59
4.21	3-dimension plots of the BER v.s. ρ for the ML decoding of STC/WFHSS for $E_b/N_J = 10$ dB with CSI available.	59

4.22 BER v.s. ρ of the ML decoding of STC/OFHSS for $E_b/N_J = 10$ dB with CSI available.	60
4.23 3-dimension plots of the BER v.s. ρ for the ML decoding of STC/OFHSS for $E_b/N_J = 10$ dB with CSI available.	60
4.24 BER v.s. ρ of the ML decoding of STC/UFHSS for $E_b/N_J = 10$ dB with CSI available.	61
4.25 3-dimension plots of the BER v.s. ρ for the ML decoding of STC/UFHSS for $E_b/N_J = 10$ dB with CSI available.	61
4.26 BER v.s. ρ for the ML and SUB1.1 decodings of the STC/WFHSS for $E_b/N_0 = 15$ dB and $E_b/N_J = 10$ dB with CSI available.	62
4.27 BER v.s. ρ for the ML and SUB2.1 decodings of the STC/OFHSS for $E_b/N_0 = 15$ dB and $E_b/N_J = 10$ dB with CSI available.	62
4.28 BER v.s. ρ for the ML and SUB3.1 decodings of the STC/UFHSS for $E_b/N_0 = 15$ dB and $E_b/N_J = 10$ dB with CSI available.	63
4.29 Performance plots of the STC/WFHSS without CSI for $\rho = 0.2$, $E_b/N_0 = 20$ dB, and JSI available.	63
4.30 Performance plots of the STC/OFHSS without CSI for $\rho = 0.2$, $E_b/N_0 = 15$ dB, and JSI available.	64
4.31 Performance plots of the STC/UFHSS without CSI for $\rho = 0.2$, $E_b/N_0 = 15$ dB, and JSI available.	64
4.32 Performance plots of the STC/WFHSS without CSI for $\rho = 0.2$ and $E_b/N_0 = 20$ dB.	65
4.33 Performance plots of the STC/OFHSS without CSI for $\rho = 0.2$ and $E_b/N_0 = 15$ dB.	65
4.34 Performance plots of the STC/UFHSS without CSI for $\rho = 0.2$ and $E_b/N_0 = 15$ dB.	66
4.35 Performance of the STC/WFHSS with CSI and JSI available for $\rho = 0.2$, $E_b/N_0 = 15$ dB and 2 receiver antennas.	66

4.36	Performance of the STC/WFHSS with CSI and JSI available for $\rho = 0.2$, $E_b/N_0 = 15$ dB and 3 receiver antennas.	67
4.37	Performance of the STC/OFHSS with CSI and JSI available for $\rho = 0.2, E_b/N_0 =$ 15 dB and 2 receiver antennas.	67
4.38	Performance of the STC/OFHSS with CSI and JSI available for $\rho = 0.2, E_b/N_0 =$ 15 dB and 3 receiver antennas.	68
4.39	Performance of the STC/WFHSS, STC/UFHSS, and STC/OFHSS systems with memory=2 and CSI available for $\rho = 0.2$ and $E_b/N_0 = 15$ dB.	68
4.40	Performance of the STC/WFHSS, STC/UFHSS, STC/OFHSS, CC/STBC/FHSS systems for $\rho = 0.2$ and $E_b/N_0 = 20dB$	69
A.1	MFSK detector.	73



List of Tables

4.1	Optimal Space-time codes of the STC/WFHSS system with 4FSK and 2 transmitter antennas for wireless jamming channels with respect to the case of low diversity.	35
4.2	Optimal Space-time codes of the STC/WFHSS system with 4FSK and 2 transmitter antennas for wireless jamming channels with respect to the case of high diversity.	35
4.3	Optimal Space-time codes of the STC/OFHSS system with 4FSK and 2 transmitter antennas for wireless jamming channels with respect to the case of low diversity.	42
4.4	Optimal Space-time codes of the STC/OFHSS system with 4FSK and 2 transmitter antennas for wireless jamming channels with respect to the case of high diversity.	43

Chapter 1

Introduction

Wireless communication systems have been used for a long time and undergone a remarkable development. The rapid growing of the wireless communication technology is driving it towards higher mobility and higher data rates. A communication system mainly consists of three components: transmitter, channel, and receiver. In general, the signals are transmitted through wireless channels in terms of electromagnetic waves from the transmitter to the receiver, and the data arrived from many different directions and with different delays cause the variations in the amplitude and phase of the composite received signals. This phenomenon is called multipath fading. Fading channels can cause a significant degradation in the performance of a communication system. Furthermore, the received signal are also affected by undesired channel impairments and some intentional and unintentional interference signals, such as, thermal noise and the signals transmitted from other users. Thermal noise is caused by the random motion of the electrons in conductors at the front end of the receiver. The signals transmitted from other users also interfere with our transmitted data. Obviously, all of these factors make the transmitted signals distortion seriously.

Conventionally, frequency-hopping spread spectrum (FHSS) systems are typically employed to mitigate the jamming effect in the wireless jamming environments [1], and are shown to provide performance improvements. The most common modulation scheme used with FH systems is the M -ary frequency-shift-keying (MFSK) modulation. The MFSK signals with FH are transmitted with a pseudo-random sequence that is used to select a set

of carrier frequency. That is, the signals are pseudo-randomly hopped over the total spread-spectrum signal bandwidth, and the jammer cannot generate the same pseudo-random numbers and frequency hopping bands used by the spread-spectrum system. For further error correction, FHSS systems usually combined with ordinary single-input single-output channel codes, e.g., Reed-Solomon (RS) [2] codes and convolutional codes (CC) [3], which are equipped for further error correction. In [4], it shows the application of RS codes to SFH/MFSK systems in wireless jamming channels. Conventionally, RS codes combined with FHSS usually use error-and-erasures decoding method to against partial-band noise [3]. In [5], Viterbi proposed the ratio threshold test as a symbol reliability measure used with RS codes to determine which code symbols should be erased before decoding. Bayesian decision theory for erasure-insertion used in FHSS system with RS codes was investigated by Baum and Pursley [6]. In [7][8], CC are combined with the noise-normalized method in FHSS systems to improve the system performance. The coded FH systems can yield much better performance than that of uncoded FH systems [3]. However, the overall performance is not satisfactory as the fading effect is considered.

The design of channel codes for providing high data rate and high quality of communications over fading channels using multiple transmitter antennas are investigated in recent years. In 1998, Tarohk, Seshadri, and Calderbank *et al* [9][10]., first proposed the space-time coding (STC) scheme, which is an effective way to approach the capacity of multiple-input multiple-output wireless channels. Space-time coding introduces a temporal and spatial correlation into the transmitted signals by using multiple antennas and has been shown to provide excellent performance against multipath fading. It can achieve transmit diversity as well as a coding gain without sacrificing the bandwidth. Generally, FHSS systems are the most effective anti-jamming communication techniques, and STC techniques can minimize the effects of multipath fading. Therefore, in this study, we combine FHSS with STC to construct a powerful transmission scheme which can effectively mitigate the effect of multipath fading and jamming interferences from spatial, temporal, and frequency domains.

The rest of this thesis is organized as follows. In Chapter 2, an overview of FHSS systems

is given, and a class of jamming environments are also introduced. In Chapter 3, STC systems including the encoding and decoding schemes and the design criteria over fading channels are introduced. In Chapter 4, STC are investigated from wireless jamming channels with respect to three kinds of FHSS systems. One is the worst-case frequency hopping which hops the symbols from all transmitter antennas into the same frequency band, another is the optimum frequency hopping which avoids any possible collision of the transmitted symbols, and the other is the uniform frequency hopping which hops the transmitted symbol randomly over the total frequency hopping bands. The actual performance of the proposed STC/FHSS system with arbitrary hopping patterns can then be upper and lower bounded by the evaluated performance of the worst case and perfect case, respectively. Moreover, the performance of the uniform case can approach the perfect case as the number of frequency bands are very large and few antennas are used for transmission. The maximum likelihood (ML) decoding together with some suboptimal schemes are presented. We also provide the performance criteria for constructing good space-time codes and show some simulation results. In Chapter 5, we conclude this thesis and propose some potential future works.



Chapter 2

Overview of Frequency-Hopping Spread Spectrum Systems and Jamming Environments

In wireless channels, the transmitted signals are distorted not only by the thermal noise of the transmitter and receiver conductor but also some intentional or unintentional jamming noises [1][11]. Generally, FHSS systems are the most effective anti-jamming communication techniques. In this chapter, we will make a simple introduction about FHSS systems and some types of jamming environments.

2.1 FHSS Systems

Spread-spectrum techniques are often used for anti-jamming [11][12]. For spread-spectrum systems, the bit signal-to-jammer noise ratio is defined as

$$\frac{E_b}{N_J} = \frac{W_s S}{R_b J} \quad (2.1)$$

where W_s is the total spread-spectrum signal bandwidth, S is the signal power at input the the intended receiver, R_b is the data rate in bits per second, $E_b = S/R_b$ is the energy per bit, J is the total fixed jammer power, and $N_J = J/W_s$ is the single-sided jammer noise power spectral density. We also defined the processing gain (PG)

$$PG = \frac{W_s}{R_b} \quad (2.2)$$

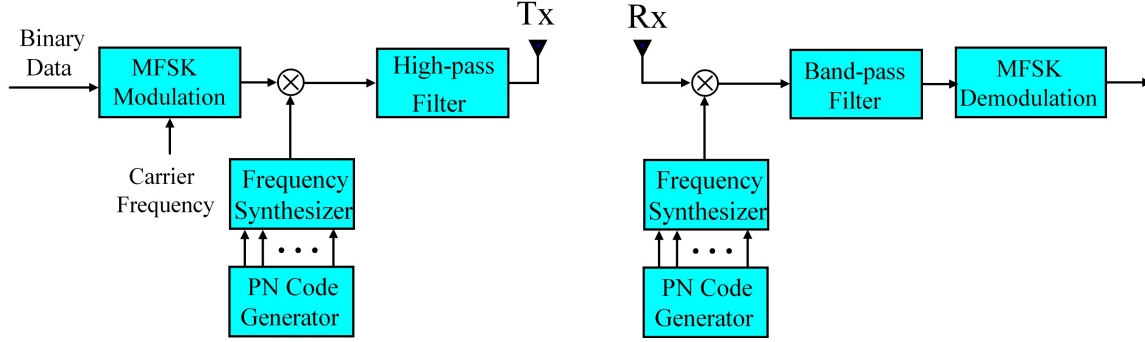


Figure 2.1: FH/MFSK system model.

and jammer-to-signal power ratio is defined as J/S . The bit signal-to-jammer noise ratio represented in decibels (dB) is

$$\frac{E_b}{N_{J(dB)}} = (PG)_{(dB)} - \left(\frac{J}{S}\right)_{(dB)}. \quad (2.3)$$

When PG becomes larger, the value of E_b/N_J is also increasing. Therefore, spread spectrum techniques could resist jammer noise effectively. Figure 2.1 illustrates the uncoded FH/MFSK systems. First of all, the binary data are fed into the MFSK modulator. Then, the modulated signal is hopped pseudo-randomly over the total system bandwidth W_s under the control of a pseudonoise (PN) sequence. Hence, the technique of FHSS systems is to change the frequency of the carrier periodically so that the jammer does not know where to jam. Current FHSS systems are classified as slow frequency hopping (SFH) and fast frequency hopping (FFH) [12]. FFH denotes the system with relatively high hop rates R_h which is an integer of the MFSK symbol rate R_s , while the SFH owns the reverse condition.

2.2 Jamming Environments

There are lots of possible jamming waveforms that could be considered to make the transmitted signals distortion. A class of jamming waveforms are selected to illustrate in this section, such as, broadband noise jammers, partial-band noise jammers, and multitone jammers [1][11].

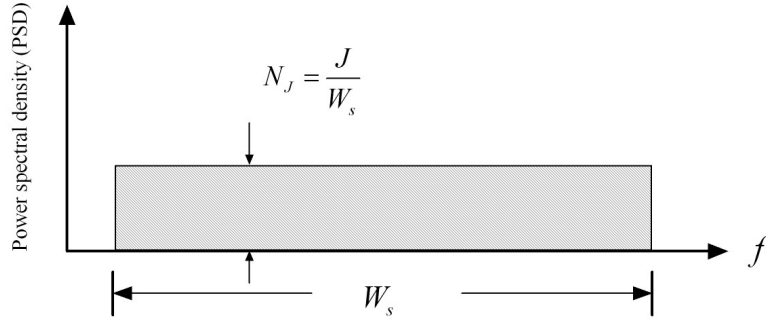


Figure 2.2: Power spectral density of broadband noise jammer.

2.2.1 Broadband Noise Jammers

A broadband noise jammer spreads its total fixed power J over the total frequency range of the system bandwidth W_s . This is equivalent to an additive white Gaussian noise (AWGN) channel with zero mean as shown in Figure 2.2, and the one-sided noise power spectral density (PSD) is

$$N_J = J/W_s. \quad (2.4)$$

In an AWGN channel, the bit error probability of a slow frequency hopping with non-coherent MFSK modulation system is

$$P_s = \frac{1}{M} \exp\left(-\frac{E_s}{2N_0}\right) \sum_{q=2}^M \binom{M}{q} (-1)^q \exp\left[\frac{E_s(2-q)}{2N_0q}\right] \quad (2.5)$$

where N_0 is one-sided power spectral density of Gaussian noise, and E_s is the energy per symbol. There are $l = \log_2 M$ bits per modulation symbol. When a symbol error occurs, the probability is equally likely to choose any of the $M-1$ incorrect orthogonal symbols. Hence, the number of bit errors corresponding to a symbol error are

$$\frac{1}{M-1} \sum_{i=1}^l \binom{M}{q} i = \frac{l2^{l-1}}{M-1} = \frac{M}{2(M-1)}l. \quad (2.6)$$

From (2.5) and (2.6), the probability of a bit error is given by

$$\begin{aligned}
 P_b &= \left[\frac{M}{2(M-1)} \right] P_s \\
 &= \frac{1}{2(M-1)} \exp\left(-\frac{lE_b}{2N_0}\right) \sum_{q=2}^M \binom{M}{q} (-1)^q \exp\left[\frac{lE_b(2-q)}{2N_0q}\right]
 \end{aligned} \tag{2.7}$$

where E_b is the energy per bit and equation (2.7) is defined as $P_b\left(\frac{E_b}{N_0}\right)$. As a broadband Gaussian noise jammer of constant power J is considered, the one-sided power spectral density of N_0 is replaced by $N_0 + N_J$. Then, the bit error probability of the FH/MFSK system could be written as

$$P_b = \frac{1}{2(M-1)} \exp\left(-\frac{lE_b}{2(N_0 + N_J)}\right) \sum_{q=2}^M \binom{M}{q} (-1)^q \exp\left[\frac{lE_b(2-q)}{2(N_0 + N_J)q}\right] \tag{2.8}$$

and it is defined as $P_b\left(\frac{E_b}{N_0 + N_J/\rho}\right)$. For the special case of $l = 1$, (2.8) becomes

$$\begin{aligned}
 P_b &= \frac{1}{2} \exp\left(-\frac{E_b}{2(N_0 + N_J)}\right) \\
 &= \frac{1}{2} \exp\left(-\frac{S/R_b}{2(N_0 + J/W)}\right).
 \end{aligned} \tag{2.9}$$

Better performance can be obtained by spread spectral to decrease N_J .

2.2.2 Partial-Band Noise Jammers

The partial-band noise jammers can be regarded as the signals which transmitted from other users and occupied a fraction of the frequency bandwidth, such as, OFDM signals, and they interfere with our transmitted data. A partial-band noise jammer restricts its total power J over the frequency range of bandwidth W_J , which is a fraction ρ ($0 \leq \rho \leq 1$) of the total system bandwidth W_s . As shown in Figure 2.3, the noise jammer spreads total power J over bandwidth $W_J = \rho W_s$, and the power spectral density of the partial-band noise jammer represents as

$$N'_J = \frac{J}{W_J} = \frac{J}{\rho W_s} = \frac{N_J}{\rho} \tag{2.10}$$

where the ratio $\rho = W_J/W_s$. Assume the partial-band noise jammer can be treated as additive Gaussian noise. Then the average error probability is

$$\bar{P}_b = (1 - \rho)P_b\left(\frac{E_b}{N_0}\right) + \rho P_b\left(\frac{E_b}{N_0 + N_J/\rho}\right) \quad (2.11)$$

where N_0 is the one-sided power spectral density of thermal noise.

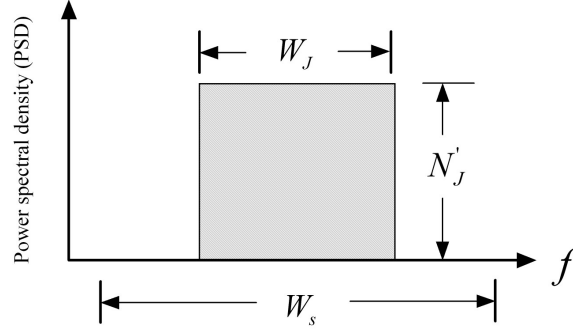


Figure 2.3: Power spectral density of partial-band noise jammer.

In general, N_J is assumed to be larger than N_0 in jamming environments, so thermal noise could be neglected. The bit error probability is simply to

$$\begin{aligned} \bar{P}_b &= \rho P_b\left(\frac{\rho E_b}{N_J/\rho}\right) \\ &= \frac{\rho}{2(M-1)} \sum_{q=2}^M \binom{M}{q} (-1)^q \exp\left[\frac{l\rho E_b(1-q)}{N_0 q}\right]. \end{aligned} \quad (2.12)$$

For a given M and E_b/N_J , the worst case partial-band noise jammer chooses ρ to maximize the \bar{P}_b . Then, the average performance from (2.12) can be expressed as

$$(\bar{P}_b)_{\max} = \max_{0 < \rho \leq 1} \left[\frac{\rho}{2(M-1)} \sum_{q=2}^M \binom{M}{q} (-1)^q \exp\left(\frac{l\rho E_b(1-q)}{N_0 q}\right) \right]. \quad (2.13)$$

Let ρ_0 denote the worst case partial-band noise jammer [11][13] and maximize the \bar{P}_b

$$\rho_0 = \begin{cases} \frac{2}{E_b/N_J}, & \text{for } \frac{E_b}{N_J} > 2 \\ 1, & \text{for } \frac{E_b}{N_J} \leq 2. \end{cases} \quad (2.14)$$

From (2.14), the maximum of \bar{P}_b is

$$(\bar{P}_b)_{\max} = \begin{cases} \frac{0.3679}{E_b/N_J}, & \text{for } \frac{E_b}{N_J} > 2 \\ \frac{1}{2} \exp\left(-\frac{E_b}{2N_J}\right), & \text{for } \frac{E_b}{N_J} \leq 2. \end{cases} \quad (2.15)$$

The performances of an FH/BFSK system in different factors ρ of partial-band noise jammers are illustrated in Figure 2.4. For small E_b/N_J , $\rho = 1.0$ which represents the broadband noise jammer is the most effective jammer. However, when E_b/N_J exceeds a threshold level, the partial-band noise jammer ($0 < \rho \leq 1$) makes the performance worst than that of the broadband noise jammer.

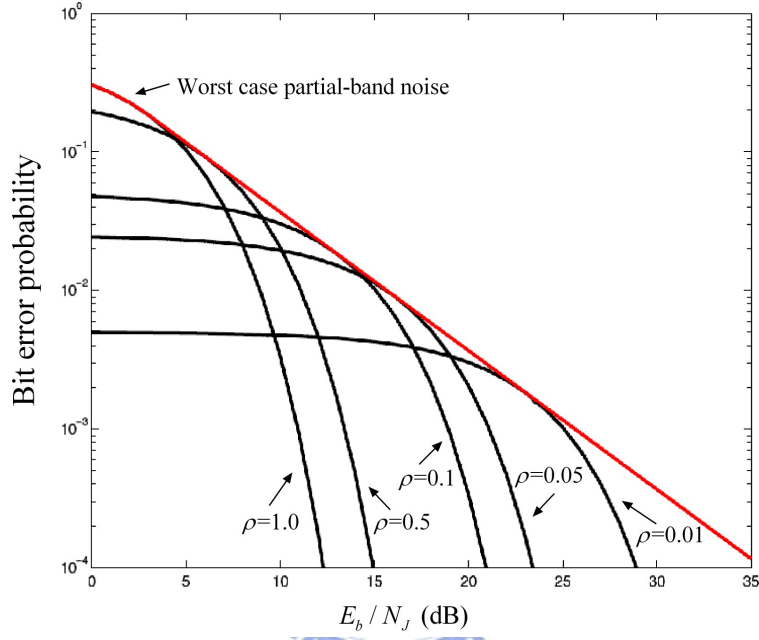


Figure 2.4: Performance of FH/BFSK system in partial-band noise jamming environment for different factors ρ

2.2.3 Multitone Noise Jammers

Multitone noise jammers can be regarded as the signals transmitted from other users, and they interfere with our transmitted data. Multitone noise jammer divides its total power J into q equal power, random phase continuous wave tones. The multitone noise jammer waveform model is

$$J(t) = \sum_{l=1}^q \sqrt{\frac{2J}{q}} \cos[\omega_0 t + \phi_l] \quad (2.16)$$

where ϕ is the random phase in $(0, 2\pi]$. Figure 2.5 illustrates the power spectral density of multiple CW tone interferences. Multitone noise jammer is sometimes more effective against FH/MFSK signals than partial-band noise jammer.

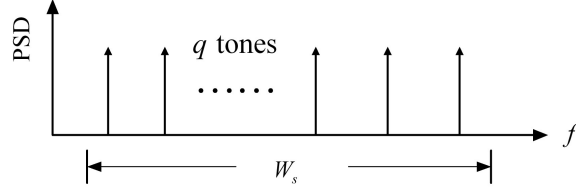


Figure 2.5: Power spectral density of multitone noise jammer.

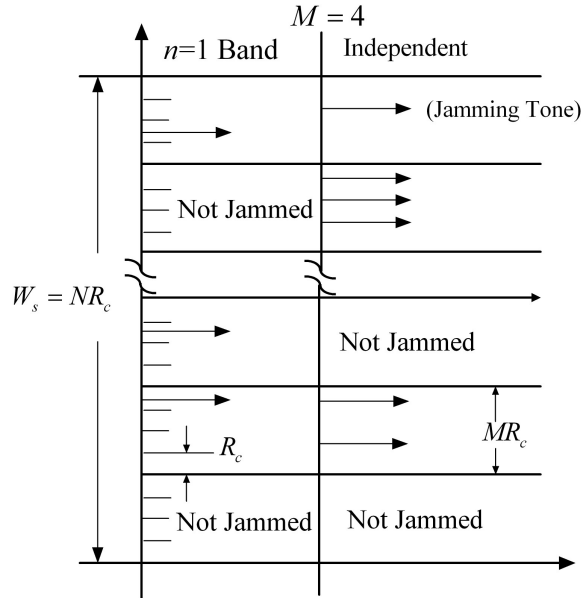


Figure 2.6: Band multitone noise jammer and independent multitone noise jammer strategies.

We assume that each jamming tone coincides exactly in frequency with at most one tone per frequency slot. In general, there are two class of multitone jamming strategies with the frequency structures for FH/MFSK systems and N tones separated by chip rate R_c as shown in Figure 2.6. One is band multitone noise jammer which places n jamming tones in each jammed M -ary band. The fraction of the jammed FH slots is defined as

$$\rho = \frac{q}{MN} \quad (2.17)$$

where N is the total frequency bands, and q is denoted the number of equal power, random phase jamming tones. The probability of n jamming signals existed in each M -ary band is defined as

$$\mu = \frac{q/n}{N}. \quad (2.18)$$

The other is called independent multitone noise jammer which is defined as q equal power jamming tones distributing over all NM FH frequency slots pseudo-randomly. The jamming noise could be independently hopped over the entire spread-spectrum bandwidth, and there is no need to determine the number of jamming tones in each M -ary band.

In order to degrade the performance of FH/MFSK systems, the jammmmer needs to find the received signal power S , and the fraction of signal to each jamming tone power is

$$\alpha = \frac{S}{J/q}. \quad (2.19)$$

Assume the jamming interference is dominated the performance of FH/MFSK systems and the receiver thermal noise could be neglected. As the data symbol is not jammed and any of the other symbols is hit with a jamming tone, an error will occur if $\alpha < 1$. On the contrary, an error will never be made if $\alpha > 1$. Therefore, choose q appropriately could determine the worst case of α and seriously degrade the performance of the FH/MFSK systems [11][14].

For slow frequency hopping, the bandwidth of a M -ary band is

$$W_b = MR_s = \frac{MR_b}{\log_2 M} = \frac{MR_b}{k} \quad (2.20)$$

where R_b is the bit rate and $R_s = R_b/\log_2 M$ is symbol rate. Then the probability of each M -ary band jammed is

$$\mu = \frac{q}{W/W_b}. \quad (2.21)$$

From (2.4), (2.19), and (2.21), and $E_b = S/R_b$, we can rewrite μ in the form

$$\mu = \frac{\alpha M}{nK E_b/N_J}. \quad (2.22)$$

If the data symbol is not hit and any of the other frequency slots is jammed in a M -ary band, the probability of symbol error for $\alpha < 1$ is

$$P_s = \mu \left(\frac{M-1}{M} \right). \quad (2.23)$$

Recalling the relation between P_s and P_b is

$$P_b = \frac{M}{2(M-1)} P_s, \quad (2.24)$$

so the probability of bit error is specified by

$$P_b = \frac{\alpha M}{2kE_b/N_J}. \quad (2.25)$$

To achieve the worst case performance by maximizing α , the condition we need is not only $\alpha < 1$ but also $\mu \neq 1$. That is, the number of jamming tones should be smaller than that of M -ary bands. The worst case band multitone jammer sets α to be

$$\alpha_{wc} = \begin{cases} \frac{kE_b}{MN_J}, & \frac{E_b}{N_J} < \frac{M}{k} \\ 1, & \frac{E_b}{N_J} \geq \frac{M}{k} \end{cases} \quad (2.26)$$

Figure 2.7 is shown that partial-band and multitone noise jammers are both significantly more effective than broadband noise against FH/MFSK signals, and the $n = 1$ band multitone jammer are the most effective jamming strategy against FH/MFSK systems.

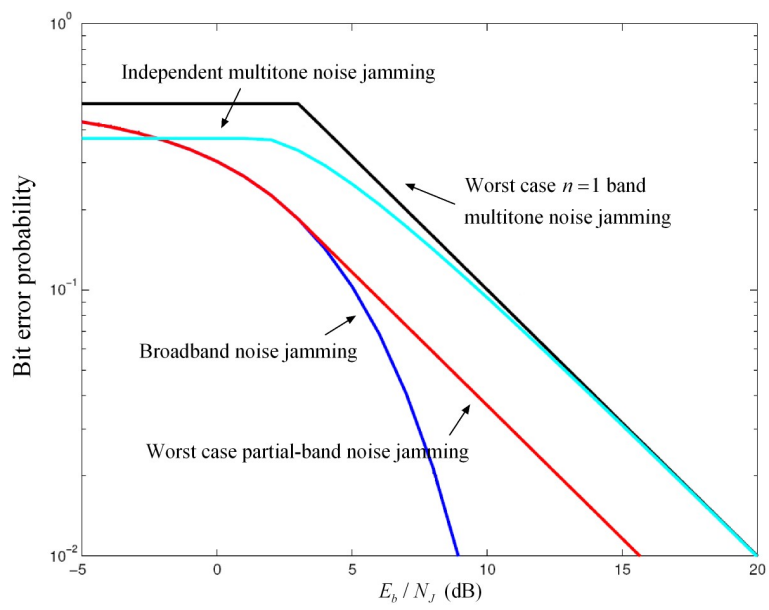


Figure 2.7: Performance of FH/MFSK in several different jamming environments.

Chapter 3

Review of Space-Time Coding

In order to increase the transmitted data rate of wireless communication systems and resist multipath fading, using multiple transmitter antennas are considered recently [15]. In 1998, Tarohk, Seshadri, and Calderbank *et al.*, first proposed the space-time coding scheme, which is an effective way to approach the capacity of multiple-input multiple-output wireless channels [9]. It introduces temporal and spatial correlation into the transmitted signals, so as to achieve transmit diversity as well as a coding gain without sacrificing the bandwidth. In this chapter, we introduce the encoding and decoding schemes of STC and the design criteria over fading channels.

3.1 STC System Model

A space-time coded communication system with n transmitter antennas and m receiver antennas as shown in Figure 3.1. First, the information bits are generated from a random source consisting of a series of zeros and ones, and then fed it into the space-time encoder.

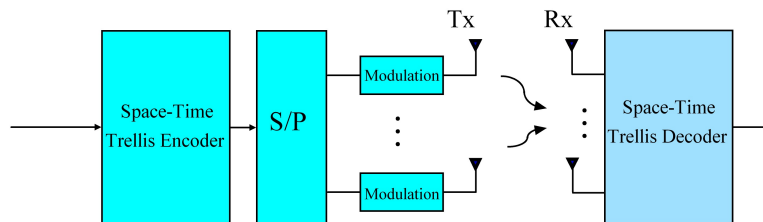


Figure 3.1: STC system model.

After encoding, the encoded data shall be divided into n codeword symbols. Then, the symbols are passed to the modulator and transmitted by n transmitter antennas. At the receiver, the signals degraded by multipath fading at each of the m receiver antennas are a superposition of the n transmitted signals with noise. Assume the wireless channels are a quasic-static flat fading and memoryless channels. Let s_t^i with energy E_s be the symbol transmitted by the i th antenna at time t . The received signal r_t^q of the q th receiver antenna at time t for all $0 \leq q \leq m, 0 \leq t \leq L$ is given by

$$r_t^q = \sum_{i=1}^n \alpha_{i,q} s_t^i \sqrt{E_s} + \eta_t^q \quad (3.1)$$

where $\alpha_{i,q}$ denotes the equivalent gain of multipath from the i th transmitter antenna to the q th receiver antenna and η_t^q stands for the AWGN. Assume $\alpha_{i,q}$ is constant during a frame L of the information sequences and vary from one frame to another. η_t^q are also assumed to be independently Gaussian distributed with zero mean and one-sided power spectral density N_0 .

There are different STC systems with respect to distinct coding schemes, such as, space-time block coding [16][17], space-time trellis coding [18][19], unitary space-time modulation [20][21], space-time turbo trellis coding [22], differential space-time coding [23][24], layered space-time coding [25][26] and space-time frequency coding [27][28], etc. In the following sections, we will focus on space-time trellis coding schemes.

3.2 Encoder Structure for STTC

Space-time trellis codes (STTC) are first provided by Tarokh, Seshadri, and Calderbank *et al.* The scheme of STTC is combined modulation and trellis coding to transmit data over multiple antennas. In addition, it is able to reduce the effects of fading. In this chapter, we discuss the 4-state space-time trellis coded with quadrature phase-shift keying (QPSK) modulation scheme and two transmitter antennas. As shown in Figure 3.2 , for example, the generator sequences are

$$(x_1^t, x_2^t) = b_{t-1}(1, 1) \oplus_4 a_{t-1}(2, 2) \oplus_4 b_t(2, 1) \oplus_4 a_t(3, 2) \quad (3.2)$$

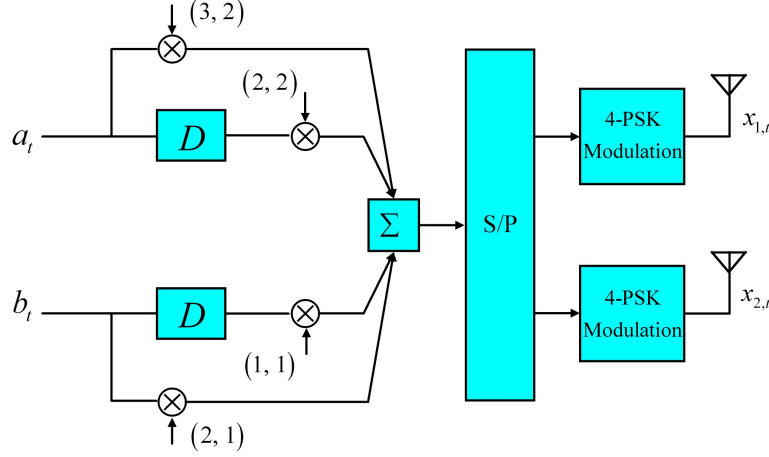


Figure 3.2: The encoder of STTC system for two transmitter antennas

where (x_1^t, x_2^t) stand for two coded QPSK symbols transmitted through antenna 1 and antenna 2, respectively. a_t and b_t represent a pair of input bits at time t . The operation of taking added modulo 4 is denoted by \oplus_4 . Assume the input sequence is $(b_t, a_t) = (1, 1)$ at time t and $(b_{t-1}, a_{t-1}) = (0, 1)$ at time $t-1$, and then the output sequence generated by (3.2) at time t is $(x_1^t, x_2^t) = (2, 0)$.

3.3 Maximum Likelihood Decoding

For STTC, the decoder performs ML decoding with respect to Viterbi algorithm. Let the receiver signals $\mathbf{r} = (r_t^q \forall q, t)$, the path gains $\boldsymbol{\alpha} = (\alpha_{i,q} \forall i, q)$, and the estimated symbols $\hat{\mathbf{s}} = (\hat{s}_t^i \forall i, t)$. Assume the $\alpha_{i,q}$'s are available at the receiver. With respect to equation (3.1), the ML decoding is given by

$$\begin{aligned}
 f(\mathbf{r}|\boldsymbol{\alpha}, \hat{\mathbf{s}}) &= \prod_{t=1}^L \prod_{q=1}^m f\left(\eta_t^q = r_t^q - \sum_{i=1}^n \alpha_{i,q} \hat{s}_t^i, \alpha_{i,q} \forall i, q, t\right) \\
 &= \prod_{t=1}^L \prod_{q=1}^m \left[\frac{1}{\sqrt{\pi N_0}} \exp\left(-\frac{|r_t^q - \sum_{i=1}^n \alpha_{i,q} \hat{s}_t^i|^2}{N_0}\right) \right].
 \end{aligned} \tag{3.3}$$

$$\tag{3.4}$$

We can drop the factors of $1/\sqrt{\pi N_0}$, $1/N_0$ in (3.4), and apply the log-domain metric:

$$\min_{\{\hat{\mathbf{s}}\}} \sum_{t=1}^L \sum_{q=1}^m \left| r_t^q - \sum_{i=1}^n \alpha_{i,q} \hat{s}_t^i \right|^2. \quad (3.5)$$

The decoding metric employs the Viterbi algorithm to select the minimum path metric as the decoded sequence.

3.4 Design Criteria for Constructing Good Space-Time Codes

We consider the space-time coded communication system with respect to ML decoding [29]. At each time t , a block of L transmitted symbols are denoted by

$$\mathbf{s} = (\mathbf{s}_1, \mathbf{s}_2, \dots, \mathbf{s}_L) \quad (3.6)$$

and the decoder selects as its estimate an erroneous sequence

$$\hat{\mathbf{s}}_t = (\hat{s}_t^1, \hat{s}_t^2, \dots, \hat{s}_t^n) \quad \forall 1 \leq t \leq L. \quad (3.7)$$

Assuming that ideal CSI is available at the receiver, and then the pairwise error probability is derived as

$$\begin{aligned} & P_{\text{R}}(\mathbf{s} \rightarrow \hat{\mathbf{s}} | \alpha_{i,j}, \forall i, j) \\ &= P_{\text{R}} \left[\sum_{t=1}^L \sum_{j=1}^m \left| r_t^j - \sum_{i=1}^n \alpha_{i,j} \sqrt{E_s} s_t^i \right|^2 \geq \sum_{t=1}^L \sum_{j=1}^m \left| r_t^j - \sum_{i=1}^n \alpha_{i,j} \sqrt{E_s} \hat{s}_t^i \right|^2 \right] \\ &= P_{\text{R}} \left[\sum_{t=1}^L \sum_{j=1}^m 2\text{Re} \left\{ \eta_t^j \sum_{i=1}^n \alpha_{i,j} \sqrt{E_s} (s_t^i - \hat{s}_t^i) \right\} \geq \sum_{t=1}^L \sum_{j=1}^m \left| \sum_{i=1}^n \alpha_{i,j} \sqrt{E_s} (s_t^i - \hat{s}_t^i) \right|^2 \right] \\ &= Q \left(\sqrt{d^2(\mathbf{s}, \hat{\mathbf{s}}) \frac{E_s}{2N_0}} \right) \end{aligned} \quad (3.8)$$

where

$$d^2(\mathbf{s}, \hat{\mathbf{s}}) = \sum_{t=1}^L \sum_{j=1}^m \left| \sum_{i=1}^n \alpha_{i,j} (s_t^i - \hat{s}_t^i) \right|^2. \quad (3.9)$$

and $Q(x)$ is the complementary error function defined by

$$Q(x) = \frac{1}{\sqrt{2\pi}} \int_x^\infty \exp(-x^2/2) dx. \quad (3.10)$$

Using the Chernoff Bound inequality

$$Q(x) \leq \frac{1}{2} e^{-x^2/2}, \forall x \geq 0. \quad (3.11)$$

The conditional pairwise error probability can be upper bounded by

$$P_{\text{r}}(\mathbf{s} \rightarrow \hat{\mathbf{s}} | \alpha_{i,j}, \forall i, j) \leq \frac{1}{2} \exp\left(-d^2(\mathbf{s}, \hat{\mathbf{s}}) \frac{E_s}{4N_0}\right). \quad (3.12)$$

Assume the fading coefficients $\alpha_{i,q}$'s are independent complex Gaussian random variables with zero mean and variance $1/2$ per dimension. Let "*" and H denote the operation of taking complex conjugate and Hermitian (transpose conjugate) respectively, and $\Omega_j = (\alpha_{1,j}, \alpha_{2,j}, \dots, \alpha_{n,j})$. Then equation (3.9) can be rewritten as

$$\begin{aligned} d^2(\mathbf{s}, \hat{\mathbf{s}}) &= \sum_{q=1}^m \sum_{i=1}^n \sum_{l=1}^n \alpha_{i,q} \alpha_{l,q}^* \sum_{t=1}^l (s_t^i - \hat{s}_t^i) (s_t^l - \hat{s}_t^l)^* \\ &= \sum_{q=1}^m \Omega_q \mathbf{B}(\mathbf{s}, \hat{\mathbf{s}}) \cdot \mathbf{B}^H(\mathbf{s}, \hat{\mathbf{s}}) \Omega_q^H \\ &= \sum_{q=1}^m \Omega_q \mathbf{A}(\mathbf{s}, \hat{\mathbf{s}}) \Omega_q^H \end{aligned} \quad (3.13)$$

where $\mathbf{B}(\mathbf{s}, \hat{\mathbf{s}})$ is defined as

$$\mathbf{B}(\mathbf{s}, \hat{\mathbf{s}}) = \begin{bmatrix} s_1^1 - \hat{s}_1^1 & s_2^1 - \hat{s}_2^1 & \cdots & s_L^1 - \hat{s}_L^1 \\ s_1^2 - \hat{s}_1^2 & s_2^2 - \hat{s}_2^2 & \cdots & s_L^2 - \hat{s}_L^2 \\ \vdots & \vdots & \ddots & \vdots \\ s_1^n - \hat{s}_1^n & s_2^n - \hat{s}_2^n & \cdots & s_L^n - \hat{s}_L^n \end{bmatrix} \quad (3.14)$$

and $\mathbf{A}(\mathbf{s}, \hat{\mathbf{s}}) = \mathbf{B}(\mathbf{s}, \hat{\mathbf{s}}) \cdot \mathbf{B}^H(\mathbf{s}, \hat{\mathbf{s}})$. Moreover, $\mathbf{A}(\mathbf{s}, \hat{\mathbf{s}})$ is nonnegative definite Hermitian, and the eigenvalues of $\mathbf{A}(\mathbf{s}, \hat{\mathbf{s}})$ are nonnegative real numbers. Therefore, we can get

$$\mathbf{V} \mathbf{A}(\mathbf{s}, \hat{\mathbf{s}}) \mathbf{V}^H = \mathbf{D} \quad (3.15)$$

where \mathbf{V} is a unitary matrix and \mathbf{D} is a real diagonal matrix. The rows of \mathbf{V} , forming a complete orthonormal basis of an N -dimensional vector space, are the eigenvectors of

$\mathbf{A}(\mathbf{s}, \hat{\mathbf{s}})$. The diagonal elements of \mathbf{D} are the eigenvalues $\lambda_i \geq 0 \forall 1 \leq i \leq n$. Next, let

$$\mathbf{\Omega}_q \mathbf{V}^H = (\beta_{1,q}, \beta_{2,q}, \dots, \beta_{n,q}). \quad (3.16)$$

Then, the equation (3.9) can be rewritten as

$$d^2(\mathbf{s}, \hat{\mathbf{s}}) = \sum_{q=1}^m \sum_{i=1}^n \lambda_i |\beta_{i,q}|^2. \quad (3.17)$$

Substituting (3.17) into (3.12), we can get

$$\Pr(\mathbf{s} \rightarrow \hat{\mathbf{s}} | \alpha_{i,q}, \forall i, q) \leq \frac{1}{2} \exp\left(-\frac{E_s}{4N_0} \sum_{q=1}^m \sum_{i=1}^n \lambda_i |\beta_{i,q}|^2\right) \quad (3.18)$$

Obviously, $\beta_{i,q}$'s are independent complex Gaussian random variables with mean $\mu_{i,q}$ and variance $1/2$ per dimension. The mean $\mu_{i,q}$ is given by

$$\begin{aligned} \mu_{i,q} &= E[\mathbf{\Omega}_q \cdot v_i] \\ &= [\mu_{\alpha,1,q}, \mu_{\alpha,2,q}, \dots, \mu_{\alpha,n,q}] \cdot v_i \end{aligned} \quad (3.19)$$

where $E[\cdot]$ denotes the expectation. Then, $|\beta_{i,q}|$ is a Rician distribution and the probability density function is

$$p(|\beta_{i,q}|) = 2 |\beta_{i,q}| \exp(-|\beta_{i,q}|^2 - \kappa_{i,q}) I_0(2 |\beta_{i,q}| \sqrt{\kappa_{i,q}}) \quad (3.20)$$

where $\kappa_{i,q} = |\mu_{\beta,i,q}|^2$ and $I_0(\cdot)$ represents the zero-order modified Bessel function of the first kind. With respect to averaging the Rician random variables $|\beta_{i,q}|$, the pairwise error probability can be expressed as

$$\begin{aligned} \Pr(\mathbf{s} \rightarrow \hat{\mathbf{s}}) &= \int_0^\infty \cdots \int_0^\infty \Pr(\mathbf{s} \rightarrow \hat{\mathbf{s}} | \beta_{i,q}, \forall i, q) p(|\beta_{1,1}|) p(|\beta_{1,2}|) \cdots p(|\beta_{n,m}|) \\ &\quad \cdot d|\beta_{1,1}| d|\beta_{1,2}| \cdots d|\beta_{n,m}| \\ &\leq \int_0^\infty \cdots \int_0^\infty \frac{1}{2} \exp\left(-\frac{E_s}{4N_0} \sum_{j=1}^m \sum_{i=1}^n \lambda_i |\beta_{i,j}|^2\right) p(|\beta_{1,1}|) p(|\beta_{1,2}|) \cdots p(|\beta_{n,m}|) \\ &\quad \cdot d|\beta_{1,1}| d|\beta_{1,2}| \cdots d|\beta_{n,m}| \\ &\leq \frac{1}{2} \prod_{q=1}^m \left(\prod_{i=1}^n \frac{1}{1 + \frac{E_s}{4N_0} \lambda_i} \exp\left(-\frac{\kappa_{i,q} \frac{E_s}{4N_0} \lambda_i}{1 + \frac{E_s}{4N_0} \lambda_i}\right) \right). \end{aligned} \quad (3.21)$$

In the case of Rayleigh fading with $\mu_{\beta,i,q} = 0$, the upper bound of the pairwise error probability becomes

$$P_{\text{r}}(\mathbf{s} \rightarrow \hat{\mathbf{s}}) \leq \frac{1}{2} \left(\prod_{i=1}^r \frac{1}{1 + \frac{E_s}{4N_0} \lambda_i} \right)^m. \quad (3.22)$$

At high SNR's, equation (3.22) can be expressed as

$$P_{\text{r}}(\mathbf{s} \rightarrow \hat{\mathbf{s}}) \leq \frac{1}{2} \left(\prod_{i=1}^r \lambda_i \right)^{-m} \left(\frac{E_s}{4N_0} \right)^{-rm}. \quad (3.23)$$

where r is the rank of $A(\mathbf{s}, \hat{\mathbf{s}})$, and λ_i 's are the non-zero eigenvalues of the matrix $A(\mathbf{s}, \hat{\mathbf{s}})$. The exponent of the SNR term, rm , is called the diversity gain and the coding gain relates to the products of eigenvalues $\prod_{i=1}^r \lambda_i$. In general, to minimize the error probability is dominated by making both diversity and coding gain as large as possible. These two criteria for designing space-time codes are called rank and determinant criteria.

